RSC Advances

ROYAL SOCIETY OF CHEMISTRY

www.rsc.org/advances

Journal Name

ARTICLE

Microfibrillated cellulose reinforced bio-based poly(propylene carbonate) with dual-responsive shape memory properties

Received 00th January 20xx,
Accepted 00th January 20xx

DOI: 10.1039/x0xx00000x

www.rsc.org/

Xiaodong Qi,[a] Mengfan Jing,[a] Zhenwei Liu,[a] Peng Dong,[a] Tianyu Liu,[a] and Qiang Fu *[a]

A novel biodegradable polymer-based composites with excellent dual-responsive shape memory properties based on poly(propylene carbonate) (PPC)/microfibrillated cellulose (MFC) was prepared. MFC was modified by a one-step mechanic-chemical approach involves ball milling and esterification reaction to improve its dispersion. The shape memory properties of PPC/MFC-BR composites and PPC/unmodified MFC composites were compared, and the former showed better shape memory properties due to the uniform dispersion of MFC-BR which ensured a higher fraction of interfacial zone than unmodified MFC. Here, MFC-BR fibers act as multifunctional cross-links, reinforcing fillers, and relaxation retarders. In addition, the composites with a MFC-BR content of 5~10 wt% showed a good shape memory effect upon exposure to water at 30 ^{o}C due to the hydrophilicity of MFC-BR. The mechanism was mainly ascribed to water molecules destroyed the hydrogen bonding at the polymer-filler interfaces, which reduced the glass transition temperature and increased the flexibility of the polymer chains. Our work provides a composite approach to tune the shape memory behavior of polymer composites and may contribute to the application of PPC in smart materials field.

1. Introduction

Shape-memory polymers (SMPs) are a class of stimuli-responsive materials that can be deformed and fixed into a temporary shape under specific stress conditions and subsequently recover their original shape upon exposure to an external stimulus, such as heat, electricity, light, magnetic field and moisture. [1-7] On the basis of such 'memorize' properties, SMPs have wide applications in various fields including textiles, packaging, aerospace and medical industries.

SMPs typically consist of two elements: switching units and netpoints. [8] The switch units are responsible for controlling shape fixity and recovery, and the netpoints determine the permanent shape of SMPs. Netpoints can be chemical in nature, as in covalently connected polymer segments in cross-linked networks. [9, 10] They can also exist as physical cross-links, as has been realized in block-copolymer-based SMPs. [11-13] It is recently supported by a number of SMPs where high content of nanoparticles are introduced in polymers to act as cross-linkers, such as the report by Xu, where SMPs based on polyhedral oligosilsesquioxane (POSS) cores are demonstrated and the work by Zhou, where hydroxyapatite (HA) act as cross-linkers are reported. [14-16]

Similarly, in our previous report, we fabricated biodegradable poly(propylene carbonate) (PPC) composites consisting of 10 wt% microfibrillated cellulose (MFC). [17] The high weight fraction of MFC-BR (MFC modified with ball milling and esterification reaction) served as physical cross-linkers and endowed the nancomposites with shape memory and self-healing properties. The key factor for achieving completely recovery is a fully cross-linked network with netpoints which are evenly distributed. [18-20] Taking such concerns into consideration, PPC/MFC-BR composites possess a more evenly filler network compared with PPC/unmodified MFC composites. However, attempts to investigate the shape memory properties of PPC/unmodified MFC composites and to compare them with PPC/MFC-BR composites have not been well studied before.

Recently, research interest into materials with water-active SMEs has been growing, because they use body fluids (mainly water) as the stimulus rather than heat. [21-25] Huang et al. found that moisture can be utilized for the water induced recovery in polyurethane SMPs. The proposed mechanism was due to the weakened hydrogen bonding between N-H and C=O groups after immersing in water. [26, 27] Hu et al. prepared cellulose/elastomer nanocomposites and found a novel water sensitivity due to the reversible hydrogen bonding among hydroxyl groups of the cellulose nano-whiskers. [28] The mechanism of the water-induce shape memory effects in these materials is a physically cross-linked network with a reversible transition of modulus triggered by water

[a] College of Polymer Science and Engineering, State Key Laboratory of Polymer Materials Engineering, Sichuan University, Chengdu 610065, China. Tel/Fax: +86-28-8546-1759. E-mail: qiangfu@scu.edu.cn

† Electronic Supplementary Information (ESI) available: [details of any supplementary information available should be included here]. See DOI: 10.1039/x0xx00000x

absorption or desorption.[21, 29, 30]

In our work, firstly, for a better understanding the importance of good filler dispersion in the shape memory polymer composites, we carried out a comparison study on the shape memory properties between PPC/MFC-BR composites and PPC/unmodified MFC composites. Secondly, it is known that MFC exhibits strong affinity towards water molecules due to its hydroxyl groups. Thus the hydrophilicity of the composites is expected to improve with the addition of MFC-BR and the water-induced shape memory behavior of PPC/MFC-BR composites is studied. The objective of the current study is to prepare biodegradable dual-responsive polymer with good shape memory property.

2. Materials and methods

2.1 Materials

Poly(propylene carbonate) (PPC) powders were supplied by the Changchun Institute of Applied Chemistry, Chinese Academy of Science (Jilin, China). Its average molecular weight (M_w) was 2.48 × 10^5 g mol^{-1}, and its M_w/M_n was 3.2. Microfibrillated cellulose (Celish MFC KY100-S) was purchased from Daicel Chemical Industries, Ltd. (Japan). N,N-Dimethylformamide (DMF) and acetyl chloride (AC) were supplied by Tianjin Bodi Chemical Co. Ltd.

2.2 Preparation of modified microfibrillated cellulose

To improve the dispersion of MFC in hydrophobic media, MFC was modified by a one-step mechanical-chemical approach involving the ball milling of MFC in DMF with an esterifying agent according to our previous report. [17] Briefly, the impregnated MFC was first homogenised in DMF using a high shear mulser at 15 000 rpm for 1 h. Next, 50 mL MFC/DMF solution (4.6 mg mL^{-1}) and 4 mL of AC were added in four dried 100 mL zirconia cylinders loaded with zirconia balls of a planetary ball mill. The mill was driven at 500 rpm under programmed punctuated operation for 8 h. The reaction mixture was cleaned by centrifugation to remove the acid and impurities followed by ultrasonication for 30 min. Hereafter, the MFC obtained by this mechanical-chemical approach is denoted as MFC-BR (modified by ball milling and reaction).

2.3 Preparation of PPC/MFC composites and PPC/MFC-BR composites

PPC (2 g) was dissolved in 20 mL DMF under vigorous stirring to yield a clear solution. Subsequently, a certain amount of MFC/DMF or MFC-BR/DMF solution was added into the PPC/DMF solution under vigorous stirring for 2 h, and the homogeneous PPC/MFC/DMF or PPC/MFC-BR/DMF solution was poured into glass frames. The casting films were dried in an air-circulating oven at 70 °C to quickly remove DMF and then dried in a vacuum oven at 60 °C for 48 h. The obtained PPC/MFC or PPC/MFC-BR composites containing 0 wt%, 5 wt%, and 10 wt% MFC or MFC-BR are denoted as PPC, PPC/MFC5, PPC/MFC10, PPC/MFC-BR5 and PPC/MFC-BR10, respectively.

2.4 Characterization

Fourier transform infrared spectroscopy (FTIR) measurements were performed on a Thermo Scientific Nicolet 6700 spectrometer (Thermo Electron Corporation) equipped with an attenuated total reflection (ATR) accessory. The chemical composition of elements was analyzed by X-ray photoelectron spectroscopy (XPS, Axis Ultra DLD, Kratos Co., UK). The dispersion of MFC and MFC-BR in PPC matrix were observed using an Olympus BX51 polarizing optical microscopy (Olympus Co., Tokyo, Japan). The dynamic mechanical behavior of PPC composites were evaluated on a dynamic mechanical analyzer (DMA Q800, TA Instruments). Stress relaxations were measured at 60 °C with the sample being strained to 50%. Tensile properties were performed on DMA at 60 °C. To investigate the shape memory behavior, a four-step program was used on DMA as follows; (1) Deforming, the sample was stretched to a strain (ε_m) with a constant force at 60 °C. (2) Fixing, the sample was then cooled to low temperature (25 °C) under a constant force. (3) Unloading, the external force was removed and recorded the strain (ε_u). (4) Recovery, the sample was reheated to 60 °C to observe the recovery process and recorded the strain (ε_p). Shape recovery ratio (R_r) and shape fixing ratio (R_f) were evaluated according to formula (1) and (2).

$$R_r = \frac{\varepsilon_m - \varepsilon_p}{\varepsilon_m} \quad (1)$$

$$R_f = \frac{\varepsilon_u}{\varepsilon_m} \quad (2)$$

The water contact angle was measured with contact angle equipment (DSA 100, KRUSS, Germany). The water uptake of the samples was calculated by measuring the samples' weight before and after the immersion in deionised water at 30 °C for 60 min. The weight ratio of absorbed water was calculated according to the following formula: $m_1 - m_0/m_0$, where m_0 is the weight of the sample before immersion in water and m_1 is the weight of the sample after immersion in water. The water content of PPC and PPC/MFC-BR composites before and after immersion in water was evaluated by thermo gravimetric analysis (TGA Q500, TA Instruments). The water-induced shape-memory behavior was measured as follows. First, the rectangular samples were folded or stretched by deforming at 60 °C and fixed by cooling to room temperature. Second, the fixed samples were immersed in water at 30 °C. Then, images of the shape recovery were recorded using a video camera. The samples were rectangular strip films with dimensions of 20 mm × 4 mm × 0.5 mm (length × width × thickness).

3. Results and discussions

3.1 Modification and characterization of MFC

MFC is a kind of bio-based material with a high aspect ratio and plenty of hydroxyl groups. Therefore, MFC aggregates easily due to physical entanglements among the fibers and the intermolecular hydrogen bonds. [31] Hence, MFC was first modified by a one-step mechanical-chemical approach. As shown in Fig. 1a, on the one hand, MFC could be physically exfoliated by the shear force caused by the rigid milling balls; on the other hand, esterification reactions could take place in the ball milling cylinders. The XPS spectrum (Fig. 1b) of MFC-BR clearly shows four components that correspond to carbon atoms in different functional groups: the non-oxygenated ring C, the C in C–O bonds, the carbonyl C, and the ester carbon (O–C=O). The peaks of carbonyl groups (C=O, 288.0 eV) and ester groups (O–C=O) confirm successful esterification reaction occurred between the hydroxyl groups and AC, which could improve the dispersion of MFC-BR in organic solvents and provide active centers for the blend with PPC. Some detailed characterization of modification can be seen in our early report. [17]

POM was employed to observe the dispersion state of MFC or MFC-BR in the PPC matrix. As shown in Fig. 1d, the white lines can be observed to be uniformly distributed throughout the sample, indicating that MFC-BR fibers are uniformly and homogenously distributed in the PPC matrix. For comparison, POM image of PPC/MFC5 is shown in Fig. 1c, the formation of MFC agglomerates within the matrix can be observed, indicating that the MFC aggregation will occur without modification. From these POM images, it is clearly proved that the modification of MFC fibers greatly improves the dispersion of MFC in the PPC matrix. MFC-BR is a one-dimensional filler with a high aspect ratio, and it easily becomes entangled with itself at high contents. These fibers interpenetrate each other, and a "MFC-BR network" structure seems to form in the PPC matrix. The formation of the filler network is usually observed in polymer nanocomposites and can be further verified via rheological methods [32]. Unfortunately, PPC is easily degraded at high temperature, and we failed to use rheological methods or transmission electron microscopy (TEM) to further confirm the formation of MFC-BR networks in the prepared composites.

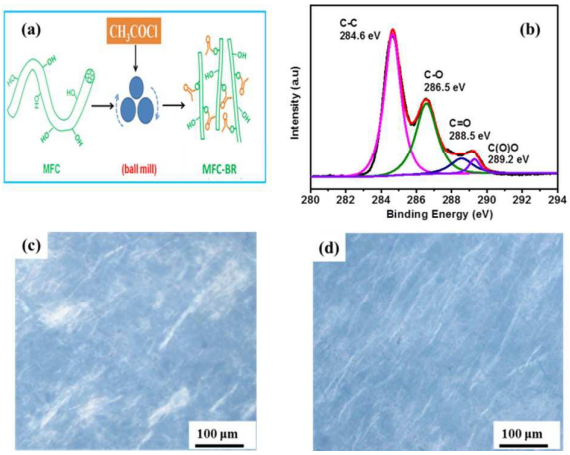

Fig. 1 (a) Scheme of MFC modified by ball milling and esterifying, (b) the C1s XPS spectra of MFC-BR. POM images of (c) PPC/MFC5 and (d) PPC/MFC-BR5.

3.2 Dynamic mechanical analysis and stress relaxations

The chain mobility for pure PPC, PPC/MFC and PPC/MFC-BR composites are investigated by DMA. Fig. 2a shows the storage modulus curves of all the samples as a function of temperature, from which one can see that the storage modulus notably increases with the addition of MFC or MFC-BR. With increasing MFC or MFC-BR content, the storage modulus curves are all right shifting, indicating a great increase of glass transition temperature (T_g). The increases in storage modulus and T_g could be attributed to the enhancement of the combined effect caused by the rigid MFC or MFC-BR fibers and the strong interactions between PPC and MFC or MFC-BR. Here it is worth noting that the storage modulus of PPC/MFC-BR10 remains about 150 MPa at 60 °C while it reduces towards zero for pure PPC, which demonstrates that there is a stiff MFC-BR network to bear the external forces loaded on the PPC/MFC-BR10. More importantly, the loss modulus peak of PPC/MFC-BR composites is higher than that of PPC/MFC composites at the same filler loading. This can be ascribed that the uniform dispersed MFC-BR ensures a higher fraction of interfacial zone within which the molecular mobility is hindered by the strong interactions between PPC and MFC-BR.

Stress relaxations have been measured to relate the relaxation phenomenon to the shape memory performance of the material (Fig. 2d). Relaxation times were defined as being the time required for the stress to decay to 1/e of the initially imposed value. [33] The measured relaxation times of PPC, PPC/MFC5, PPC/MFC10, PPC/MFC-BR5 and PPC/MFC-BR10 are 120, 156, 228, 450 and 1200 s, respectively. This effect of filler addition agrees with the results of a previous study that reported an increased relaxation time with the incorporation of well-dispersed silica particles. [33] Basic requirement for shape-memory effect is that no polymer chain relaxation (slipping, contraction, or flow) under stress during the programming stage. [1] Most polymer chains of PPC and PPC/MFC composites are relaxed during stretching, but not of PPC/MFC-BR composites. Therefore, PPC/MFC-BR composites are expected to exhibit much improved recovery over PPC and PPC/MFC composites due to their longer relaxation time and the uniform dispersed MFC-BR network.

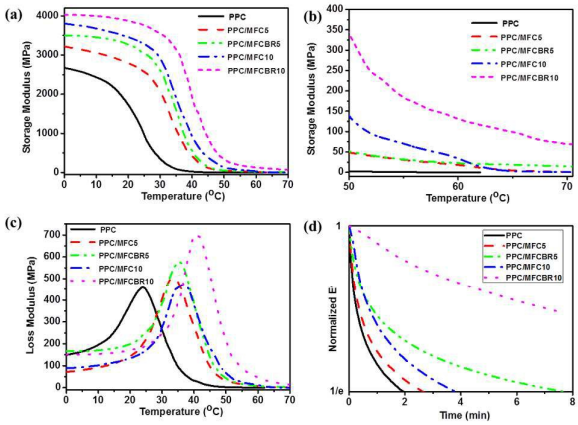

Fig. 2 DMA curves of pure PPC, PPC/MFC and PPC/MFC-BR composites (5%, 10%). (a) Storage modulus as a function of temperature. (b) The magnification of curves in the temperature range of 50-70 °C. (c) Loss modulus as a function of temperature. (d) Stress relaxation of PPC, PPC/MFC and PPC/MFC-BR composites (5%, 10%).

3.3 Mechanical properties of PPC/MFC and PPC/MFC-BR composites

It is also of great importance to evaluate the tensile properties of composites above T_g because an external force will be loaded to achieve its temporary shape. [34] Thus, tensile testing is carried out at 60 °C with DMA, and the result is shown in Fig. 3. The tensile strength of pure PPC is only 1 MPa at such a high temperature. The chains of PPC are in the rubbery state and can be easily removed by external forces, resulting in lower mechanical strength but significantly enhanced elongation (broken at 500%). For PPC/MFC5 and PPC/MFC-BR5, the tensile strength increases to 4.5 MPa and 4 MPa, respectively, combined with decreases in elongation. When MFC or MFC-BR content increases to 10 wt%, the tensile strength is further improved to above 6 MPa for PPC/MFC10 and PPC/MFC-

BR10, but the elongation decreases to 200% or even less. It is known that the poor high-temperature mechanical properties of PPC restrict its practical application. [17, 35, 36] The PPC/MFC composites prepared in this study have the potential to be used as materials at high temperature. It should be noted that the strain at broken and elastic strain energy (area under the stress-strain curve) of PPC/MFC-BR composites are larger than those of PPC/MFC composites at the same filler loading. This can be ascribed to the aggregation of MFC fibers would disturb the chain motions and impede the elastic properties of PPC. [17]

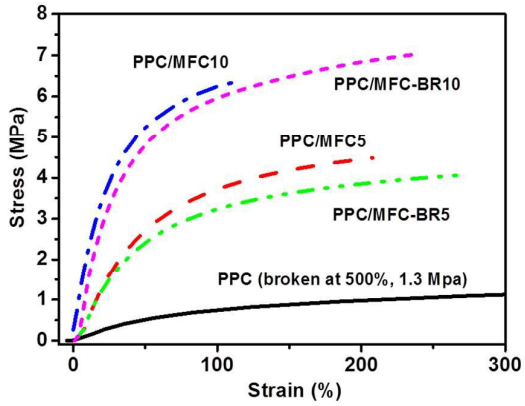

Fig. 3 Tensile behaviors of PPC, PPC/MFC and PPC/MFC-BR composites (5%, 10%) at 60 °C.

3.4 Shape memory properties of PPC/MFC and PPC/MFC-BR composites

Previous studies suggest that ensuring the uniform distribution of fully cross-linked netpoints is the key factor for achieving complete recovery. [18, 19, 33] In our work, the uniform dispersion of MFC-BR and its high weight fraction ensure a higher fraction of interfacial zone than unmodified MFC. The relaxation time increases tremendously when the MFC-BR fibers are introduced into the PPC matrix. Consequently, PPC/MFC-BR composites are expected to exhibit much improved recovery over PPC and PPC/MFC composites. Fig. 4 shows the shape memory behaviors of PPC, PPC/MFC and PPC/MFC-BR composites. Pure PPC shows relatively poor R_f and R_r, due to the low rubbery modulus of PPC at room temperature and rapid chain relaxation during the programming stage. With the simple addition of MFC to PPC, the shape fixity increases and the shape recovery remains almost constant. It is worth to note that when adding 5 wt% or 10 wt% MFC-BR, R_f and R_r both increase to nearly 95% (Fig. 4c and e). The PPC/MFC-BR composites show better shape memory performances than the PPC/MFC composites. For PPC/MFC, MFC aggregates easily, which would disturb the chain motions and impede the elastic properties of PPC. On the other hand, the simultaneous use of both mechanical and chemical methods allows the excellent dispersion of MFC-BR in PPC matrix. The uniform dispersed MFC-BR could react with a large amount of PPC molecules and generate sufficient interfacial interactions, which serve as physical cross-linking points, retard chain relaxation and augment the amount of frozen strain during loading and cooling. This is especially true for cross-linked SMPs, where less relaxed networks induce high retraction force and good shape recovery. [19, 20, 33]

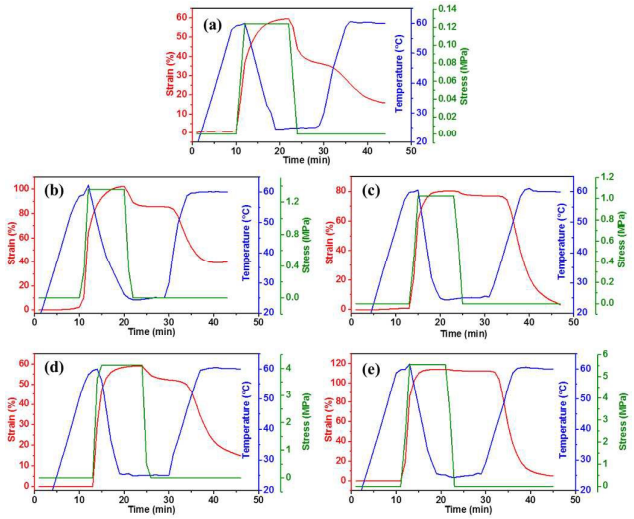

Fig. 4 The thermal-mechanical tensile curves of of PPC, PPC/MFC and PPC/MFC-BR composites, (a) PPC, (b) PPC/MFC5; (c) PPC/MFC-BR5; (d) PPC/MFC10; (e) PPC/MFC-BR10.

3.5 Hydrophilicity of PPC/MFC-BR composites

It is known that PPC is a typically hydrophobic polymer and MFC exhibits strong affinity towards water molecules due to its hydroxyl and carboxyl groups. [24, 37] The hydrophilicity of the composites is expected to be improved with the addition of MFC or MFC-BR. To verify the change in the hydrophilicity of the PPC composites after adding MFC or MFC-BR, the water contact angle was measured. As shown in Fig. 5, pure PPC shows a contact angle of 68° in water, whereas the water contact angles of the PPC/MFC10 and PPC/MFC-BR10 composites decreases to 48° and 35°, respectively. This result indicates that the wettability of PPC is improved due to the great hydrophilicity of MFC, which features an abundance of surface hydroxyl groups [24]. It's interesting to note that the water contact angel of PPC/MFC-BR composites is lower than that of PPC/MFC composites at the same filler loading. Actually, MFC should be more hydrophilic than MFC-BR due to its more surface hydroxyl groups. The improvement of hydrophilicity may be ascribed to the uniform dispersion of MFC-BR which ensures more water absorption points. We have claimed that PPC/MFC-BR composites exhibit much improved recovery over PPC and PPC/MFC composites in above discussion. Thus, the water-induced shape memory behavior and mechanism of only PPC/MFC-BR composites are studied in following parts.

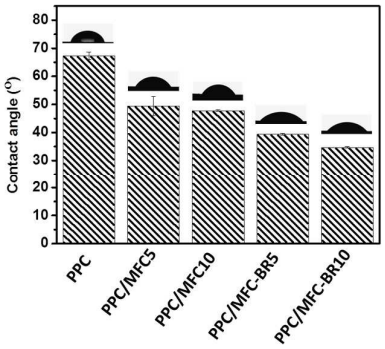

Fig. 5 Water contact angle of PPC, PPC/MFC and PPC/MFC-BR composites (5%, 10%).

3.6 Water-induced shape-memory effect of PPC/MFC-BR composites

Fig. 6 shows the water-induced shape-recovery behavior of the pure PPC and PPC/MFC-BR composites in the dry or wet state. The straight (original shape) specimens were bent into "U" like shape or stretched (temporary shape) at 60 °C and retained this shape with external load during cooling back to room temperature (25 °C). The deformed samples were immersed in water at 30 °C and the momentary shape was recorded using a digital camera at different time intervals in the whole recovery process. It can be observed that all of the samples retained their temporary shape and showed no shape recovery in the dry state at 25 °C; however, when immersed in water at 30 °C, PPC/MFC-BR composites with 5 wt% and 10wt% MFC-BR exhibited good shape recovery behavior under the stimulus of water at 30 °C for 60 min. It should be noted that no apparent shape recovery was observed after the deformed PPC/MFC-BR strips were left in air at 30 °C for 5 hours until it was immersed in 30 °C water, which indicates that the samples could not recover their initial shape at 30 °C without the stimulus of water. In addition, after the samples were immersed into water for 60 min at 30 °C, no noticeable expansion in volume was found along with the shape recovery in PPC/MFC-BR composites, which was different from PVA/GO nanocomposites in our previous study. [22] To better validate and qualitatively identify the mechanism of shape recovery in PPC/MFC-BR composites actuated by water, a systematic study on the effects of water to the PPC/MFC-BR composites was carried out.

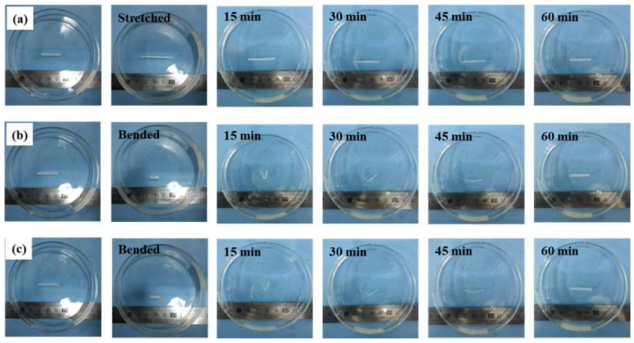

Fig. 6 The shape memory effect of PPC/MFC-BR5 (a, stretched; b, bended) and PPC/MFC-BR10 (c, bended) in water at 30 °C.

3.7 Water absorption analysis PPC/MFC-BR composites

Fig. 7a displays the water fraction in weight % in the PPC matrix as a function of immersion time at 30 °C. It can be observed that the pure PPC exhibited no water absorption due to its high hydrophobicity, whereas the PPC/MFC-BR composites absorbed more and more water with increasing MFC-BR content. The composites tended to reach their saturated state after 50 min of immersion in water. Finally, the maximum absorbed water content of 4% was obtained for PPC/MFC-BR10. The increased hydrophilcity of PPC is due to the introduction of hydrophilic MFC-BR fibers. Fig. 7b, c, d reveal the TGA curves of PPC and PPC/MFC-BR composites before and after immersion in water at 30 °C for 60 min. Pure PPC starts to decompose at about 200 °C, as evidenced by the rapid decrease in weight. The initial thermal decomposition temperature of PPC increases with the addition of MFC-BR for MFC-BR can effectively prevent heat transfer in the composites, resulting in the improvement of the heat resistant properties. Before decomposition, pure PPC shows no obvious weight loss after immersion due to its high hydrophobicity. However, PPC/MFC-BR composites that have been immersed in water lose dramatic amount of weight from 50 °C to 150 °C. This should be the result of the evaporation of the absorbed water in PPC. For convenience, the weight fraction at 150 °C is chosen as the reference for comparison. The weight loss of PPC/MFC-BR composites with 5% and 10% MFC-BR at 200 °C are 3 wt%, 4 wt%, respectively. The side hydroxyl groups and carbonyl groups of MFC-BR have the ability to connect with water molecules via formation of hydrogen bonds. [24, 28] The higher content of MFC-BR triggers more water molecules to become involved in hydrogen bonding. As expected, weight loss becomes significant with the increase of MFC-BR.

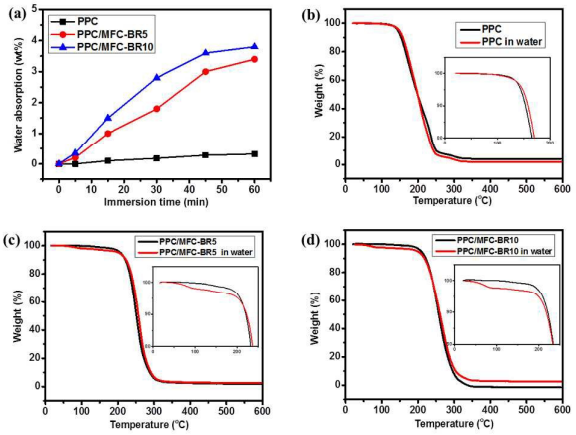

Fig. 7 (a) Ratio of absorbed water to sample weight as a function of immersion time. TGA curves of PPC/MFC-BR composites before and after immersion in water for 60 min, (b) Pure PPC, (c) PPC/MFC-BR5, (d) PPC/MFC-BR10.

3.8 Effect of water on the modulus and T_g of PPC/MFC-BR composites

The effect of water absorption on the storage modulus and T_g of PPC was also investigated using DMA analysis. Fig. 8 shows the DMA results of pure PPC and PPC/MFC-BR composites before and after immersion in water at 30 °C for 30 and 60 min. Pure PPC shows little difference on the storage modulus and T_g after immersion in water for 60 min. It indicates water molecules have little influence on PPC due to its high hydrophobicity. However, the storage modulus and T_g of PPC/MFC-BR composites decrease obviously after immersion in water for 30 min. When the samples were immersed in water for 60 min, the decline in storage modulus and T_g become more significant. In addition, PPC/MFC-BR5 immersed in water for 30 min and 60 min shows two transitions, which indicates that the water penetration mode is in a gradual manner. [22, 38] From these DMA results, it reveals that the T_g of the immersed PPC/MFC-BR composites is lowered and samples become rubber-like after immersion in water for 60 min. The result provides

evidence to support some previous statement that SMPs imbibe solvent molecules, resulting in the decline of the switching temperature and the interactive forces among tangled polymer chains. [21, 22, 39, 40]

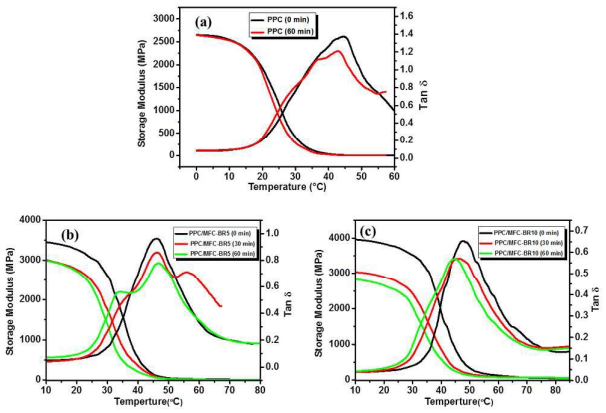

Fig. 8 DMA curves of PPC/MFC-BR composites before and after immersion in water for 30 min, 60 min; (a) Pure PPC, (b) PPC/MFC-BR5, (c) PPC/MFC-BR10.

3.9 Interactions of water with PPC/MFC-BR composites

At this point, we have demonstrated that water has a strong depressed influence on the storage modulus and T_g of PPC/MFC-BR composites, leading to the shape recovery. FTIR spectroscopy was used to study the possible interactions between PPC/MFC-BR composites and water molecules. Fig. 9 presents the full FTIR spectra of PPC/MFC-BR composites before and after immersion in water for 60 min. The peaks of -OH (3273 cm^{-1}) and C=O (1730 cm^{-1}) bonds that are relevant to this study are identified. The infrared band of the C=O stretching from PPC matrix doesn't shift to a lower or higher frequency. It indicates that PPC has little interaction with water molecules, which is consistent with above TGA and DMA analysis. For pure PPC, the absorption band located at 3530 cm^{-1} increases slightly in the wet state and this can be attributed to the presence of a small amount of unassociated water. [28] On the other hand, the intensity of the wide peak of -OH stretching from MFC-BR weakens after immersion in water for 60 min. Moreover, the intensity of -OH stretching decreases more apparently when MFC-BR content is 10 wt%, which indicates that more -OH groups involved in hydrogen bonding with water. Therefore, the FTIR results reveal that the presence of MFC-BR in the PPC has a large effect on the absorption of water that interacts with MFC-BR, which largely weakens the primary interactions in the PPC/MFC-BR composites. In this case, the competitive interactions among PPC, MFC-BR fibers and water are the main factors for the decline of the storage modulus and T_g, rather than the plasticizing effect to some extent. [22, 28, 41]

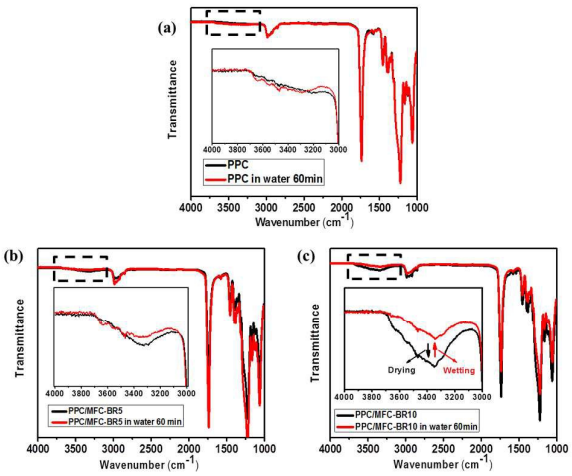

Fig. 9 FTIR results of PPC/MFC-BR composites before and after immersion in water for 60 min, (a) Pure PPC, (b) PPC/MFC-BR5, (c) PPC/MFC-BR10.

3.10 Mechanism of the shape-memory effect for PPC/MFC-BR composites

To give a vivid description of the dual responsive shape recovery of PPC/MFC-BR composites, three sketches are drawn according to the above discussions (Fig. 10). During fabrication of PPC/MFC-BR composites, MFC is first modified by a one-step mechanical-chemical approach involving ball milling and esterification reaction. The high weight fraction of MFC-BR and its uniform dispersion ensure a higher fraction of interfacial zone than unmodified MFC. The PPC/MFC-BR composites with long relaxation times can prohibit polymer chain relaxation during the programming step, resulting in high shape fixity and high shape recovery. Here, MFC-BR fibers act as multifunctional cross-links, reinforcing fillers, and relaxation retarders, which greatly improve the shape memory property of PPC. The wettability of the PPC matrix is improved due to the great hydrophilicity of MFC-BR, which features an abundance of surface hydroxyl and carbonyl groups. The observation in this study demonstrates that besides heat stimulus, water can be used as another driving force for PPC/MFC-BR composites. It's known that water molecules can act as both the donor and the acceptor for hydrogen bonds in the composite structure, forming a co-operative hydrogen bond network composed of weak water and MFC-BR interactions to replace the strong interactions of PPC and MFC-BR. [41] Water molecules destroy the hydrogen bonding at the polymer-filler interfaces, leading to the decline of the storage modulus and T_g. The effect of decrease in internal energy is analogical to the increase in temperature on the recovery of SMPs. When the switching

temperature of SMPs arrives at 30 °C or lower, the recovery is therefore induced, resulting from the released strain energy which is stored in SMPs. [40, 42]

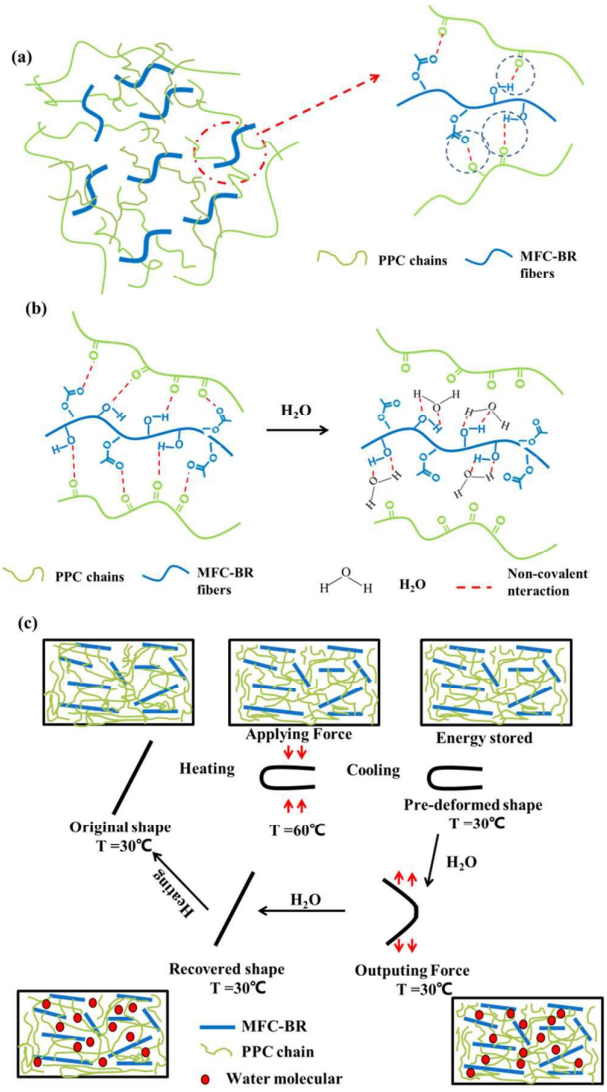

Fig. 10 (a) Schematic illustration of the interactions between PPC with MFC-BR fibers. (b) Illustration of competitive interactions among PPC, MFC-BR fibers and water, and (c) schematic representation of the shape memory behavior actuated by water.

4 Conclusions

In this study, we successfully prepared biodegradable polymer-based composites with excellent dual-responsive shape memory properties. By using a chemical-co-physical approach, a high content of MFC-BR (up to 10 wt%) was incorporated into PPC with excellent dispersion. PPC/MFC-BR composites and PPC/unmodified MFC composites were compared, and the former showed better shape memory properties due to the uniform dispersion ensure a higher fraction of interfacial zone than unmodified MFC. Here, MFC-BR fibers act as multifunctional cross-links, reinforcing fillers, and relaxation retarders. The composites with a MFC-BR content of 5~10 wt% showed a good shape memory effect upon exposure to water at 30 °C due to the hydrophilicity of MFC-BR. The mechanism is such that water molecules destroy the hydrogen bonding at the polymer-filler interfaces, which reduces the T_g and increases the flexibility of the polymer chains. Therefore, the water-induced shape memory composite can potentially be developed into a smart medical device.

Acknowledgements

This work was supported by the National Natural Science Foundation of China (51421061 and 51210005)

Notes and references

1. A. Lendlein and S. Kelch, *Angew. Chem., Int. Ed.,* 2002, **41**, 2034.
2. C. Liu, H. Qin and P. T. Mather, *J. Mater. Chem.*, 2007, **17**, 1543.
3. J. Hu, Y. Zhu, H. Huang and J. Lu, *Prog. Polym. Sci.*, 2012, **37**, 1720.
4. Q. Zhao, H. J. Qi and T. Xie, *Prog. Polym. Sci.*, 2015, **49-50**, 79.
5. Y. Liu, H. Lv, X. Lan, J. Leng and S. Du, *Compos. Sci. Technol.,* 2009, **69**, 2064.
6. S. Rana, J. W. Cho and L. P. Tan, *RSC Advances*, 2013, **3**, 13796.
7. M. Huang, X. Dong, L. Wang, J. Zhao, G. Liu and D. Wang, *RSC Advances*, 2014, **4**, 55483.
8. T. Xie, *Polymer*, 2011, **52**, 4985.
9. T. Xie and I. A. Rousseau, *Polymer*, 2009, **50**, 1852.
10. C. D. Liu, S. B. Chun, P. T. Mather, L. Zheng, E. H. Haley and E. B. Coughlin, *Macromolecules*, 2002, **35**, 9868.
11. A. Lendlein and R. Langer, *Science*, 2002, **296**, 1673.
12. B. S. Lee, B. C. Chun, Y.-C. Chung, K. I. Sul and J. W. Cho, *Macromolecules*, 2001, **34**, 6431.
13. S. Thakur and N. Karak, *RSC Advances*, 2013, **3**, 9476.
14. J. Xu and J. Song, *Proc. Natl. Acad. Sci. U. S. A.,* 2010, **107**, 7652.
15. X. Zheng, S. Zhou, X. Li and J. Weng, *Biomaterials*, 2006, **27**, 4288.
16. S. B. Zhou, X. T. Zheng, X. J. Yu, J. X. Wang, J. Weng, X. H. Li, B. Feng and M. Yin, *Chem. Mater.*, 2007, **19**, 247.
17. X. D. Qi, G. H. Yang, M. F. Jing, Q. Fu and F. C. Chiu, *J. Mater. Chem. A*, 2014, **2**, 20393.
18. K. Du and Z. Gan, *J. Mater. Chem. B*, 2014, **2**, 3340.
19. Y. Zhang, Q. Wang, C. Wang and T. Wang, *J. Mater. Chem.*, 2011, **21**, 9073.
20. Y. Bai, C. Jiang, Q. Wang and T. Wang, *Carbohydr. Polym.*, 2013, **96**, 522.
21. H. Du and J. Zhang, *Soft Matter*, 2010, **6**, 3370.
22. X. Qi, X. Yao, S. Deng, T. Zhou and Q. Fu, *J. Mater. Chem. A*, 2014, **2**, 2240.
23. L. Wang, X. Yang, H. Chen, G. Yang, T. Gong, W. Li and S. Zhou, *Poly. Chem.*, 2013, **4**, 4461.
24. Y. Liu, Y. Li, H. Chen, G. Yang, X. Zheng and S. Zhou, *Carbohydr. Polym.*, 2014, **104**, 101.
25. Y. Liu, Y. Li, G. Yang, X. Zheng and S. Zhou, *ACS. Appl. Mater. Interfaces*, 2015, **7**, 4118.

26. W. M. Huang, B. Yang, Y. Zhao and Z. Ding, *J. Mater. Chem.*, 2010, **20**, 3367.
27. W. M. Huang, B. Yang, L. An, C. Li and Y. S. Chan, *Appl. Phy. Lett.*, 2005, **86**, 114105.
28. Y. Zhu, J. Hu, H. Luo, R. J. Young, L. Deng, S. Zhang, Y. Fan and G. Ye, *Soft Matter*, 2012, **8**, 2509.
29. T. Wu, M. Frydrych, K. O'Kelly and B. Chen, *Biomacromolecules*, 2014, **15**, 2663.
30. T. Wu, K. O'Kelly and B. Chen, *Eur. Polym. J.*, 2014, **53**, 230.
31. P. Huang, M. Wu, S. Kuga, D. Wang, D. Wu and Y. Huang, *ChemSusChem*, 2012, **5**, 2319.
32. D. Wu, Y. Zhang, M. Zhang and W. Yu, *Biomacromolecules*, 2009, **10**, 417.
33. D. H. Jung, H. M. Jeong and B. K. Kim, *J. Mater. Chem.*, 2010, **20**, 3458.
34. Z. Tang, D. Sun, D. Yang, B. Guo, L. Zhang and D. Jia, *Compos. Sci. Technol.,* 2013, **75**, 15.
35. J. Gao, H. Bai, X. Zhou, G. Yang, C. Xu, Q. Zhang, F. Chen and Q. Fu, *Nanotechnology*, 2014, **25**, 025702.
36. G. Yang, C. Geng, J. Su, W. Yao, Q. Zhang and Q. Fu, *Compos. Sci. Technol.,* 2013, **87**, 196.
37. X. Hu, C. Xu, J. Gao, G. Yang, C. Geng, F. Chen and Q. Fu, *Compos. Sci. Technol.,* 2013, **78**, 63.
38. B. Yang, W. M. Huang, C. Li and L. Li, *Polymer*, 2006, **47**, 1348.
39. W. Wang, H. Lu, Y. Liu and J. Leng, *J. Mater. Chem. A*, 2014, **2**, 5441.
40. H. Lu, Y. Liu, J. Leng and S. Du, *Eur. Polym. J.,* 2010, **46**, 1908.
41. J. Chen, Y. Gao, W. Liu, X. Shi, L. Li, Z. Wang, Y. Zhang, X. Guo, G. Liu, W. Li and B. D. Beake, *Carbon*, 2015, **94**, 845.
42. H. B. Lv, J. S. Leng, Y. J. Liu and S. Y. Du, *Adv. Eng. Mater.*, 2008, **10**, 592.